A Comparative Study of Two Shadow Fading Models in Ultrawideband and Other Wireless Systems

Ali Abdi[1], *Senior Member, IEEE,* and Mostafa Kaveh[2], *Fellow, IEEE*

[1]Dept. of Elec. and Comp. Eng., New Jersey Institute of Technology, Newark, NJ 07102, USA
[2]Dept. of Elec. and Comp. Eng., University of Minnesota, Minneapolis, Minnesota 55455, USA

Contact Email: ali.abdi@njit.edu

Abstract - The distribution of the local average power at a mobile is usually considered to be lognormal in terrestrial and satellite channels. However, the mathematical form of the lognormal distribution is not convenient for analytic calculations. In this paper, we show the utility of the gamma distribution for shadow fading, in both terrestrial and satellite channels, using empirical data. Furthermore, we show that the application of the gamma model of shadow fading results in closed-form and mathematically-tractable solutions for key system performance measures such as the average symbol error rate of different modulations with a variety of diversity combining techniques.

Keywords: Shadow Fading, Shadowing, Lognormal Distribution, Gamma Distribution, Fading Channels, Large-Scale Fading, Performance Analysis.

This work was presented at IEEE Vehicular Technology Conference, Houston, TX, 1999, and Atlantic City, NJ, 2001. It was supported in part by NSF, under the Wireless Initiative Program, Grant #9979443.

I. INTRODUCTION

The local average power of the signal at the mobile station (MS), the instantaneous power averaged over a distance of a few wavelengths, fluctuates randomly from place to place in a mobile radio channel. This phenomenon is generally referred to as shadow fading. The probability density function (PDF) of the local average power is widely accepted to be lognormal for both terrestrial channels [1] and satellite channels [2]. However, the mathematical form of the lognormal PDF is not convenient for the analytic calculations that arise in connection with shadow fading in wireless channels. In fact, with the lognormal model of shadow fading, we cannot obtain closed-form and easy-to-use expressions for many performance measures of interest such as the average symbol error rate of different modulation schemes with a variety of diversity combining techniques [3], outage probability in the presence of multiple cochannel interferers [1], and so on. The complicated closed form average bit error rate expression for the simple binary phase shift keying (BPSK) modulation with a single antenna receiver [4] is a good example of the intractability of analytic calculations with the lognormal PDF. Even the numerical integration of the expressions involving the lognormal PDF using the Hermite method of integration is not a straightforward procedure and one should carefully control the error using another technique such as the Simpson integration rule [5].

In this paper, we first demonstrate the utility of the gamma PDF for shadow fading in terrestrial and satellite channels using empirical data. For terrestrial channels, we employ the data collected in urban and suburban areas [6], as well as the empirical parameters given in [1] and [7], whereas for satellite channels we use the extensive empirical information published in [8]. We then show how the application of the gamma PDF, in conjunction with the Rayleigh model of multipath fading, results in closed-form expressions for key system performance measures in both terrestrial and satellite channels.

II. DATA ANALYSIS

Let R denote the envelope of the narrowband received signal. Let S_0 represent the local average power of the envelope, i.e., $S_0 = E[R^2 | S_0]$. For the gamma model of shadow fading we have

$$f_{S_0}(s_0) = \left(\frac{\nu}{\Omega}\right)^{\nu} \frac{s_0^{\nu-1}}{\Gamma(\nu)} \exp\left(\frac{-\nu s_0}{\Omega}\right), \quad s_0 \geq 0, \tag{1}$$

where $\Gamma(.)$ is the gamma function, and $\nu = \left(E[S_0]\right)^2 / Var[S_0]$ and $\Omega = E[S_0]$ are the shape and scale parameters, respectively, with *Var*[.] as the variance. The PDF of the lognormal model is

$$f_{S_0}(s_0) = \frac{1}{\sqrt{2\pi\sigma^2}\, s_0} \exp\left[\frac{-(\ln s_0 - \mu)^2}{2\sigma^2}\right], \quad s_0 \geq 0, \tag{2}$$

where $\mu = E[\ln S_0]$, $\sigma^2 = Var[\ln S_0]$, and $\ln(.)$ is the logarithm to the base *e*. In addition to the references given in [9], some other physical/statistical explanations for the gamma distribution of S_0 can be inferred from [10], [11], and [12]. The interesting property of the gamma distribution discussed in [13] may open up another door to the justification of this model for shadow fading.

A. Terrestrial Channels

A typical envelope record, $R(t)$, out of twelve terrestrial channel measurements [6] is shown in Fig. 1[1]. The square root of the running mean of the envelope squared, $\sqrt{S_0(t)}$, is also shown on the same graph. The length of the sliding temporal window was 1 second, equivalent to a spatial window of length 20λ, with λ as the wavelength of a 910 MHz carrier. As is discussed in [17], the length of the sliding window has little effect of the histogram of $S_0(t)$

---

[1] More details about the collected data, the locations, and other statistical characteristics of the data can be found in [14], [15], and [16]. Two sites were used for the collection of data: a suburban housing development in Greenville, Texas, and an urban area among the buildings of the campus of the University of Texas at Arlington. In the suburban area, parked vehicles, vegetation, and inconsistency in the setback of the housing structures produced very irregular reflective conditions. The urban environment was characterized by buildings of one to six stories in height, heavy traffic, large open areas, and highly inconsistent setback from the street.

(18λ and 26λ are compared in [17] at 836 MHz). In order to compare the empirical distribution of $S_0(t)$ with gamma and lognormal models, we use statistical goodness-of-fit tests [18] and information-theoretic approaches [19].

A.1. Cramer-von Mises Test

The Kolmogorov-Smirnov (KS) and Pearson's chi-square (PCS) tests are two common tests that have been widely used in studying the goodness-of-fit of a variety of fading distributions to channel measurements. Some common pitfalls regarding the KS and PCS tests are discussed in [21] and [22]-[23], respectively. According to the nature of $S_0(t)$, KS test is a better choice as it is directly applicable to ungrouped continuous data, while the inevitable grouping of the data in the PCS test, which can be done in many different ways, discards some information [24]. However, since the power of the KS test (the probability of accepting the alternative hypothesis when the alternative hypothesis is true) is small [25], we use the more powerful Cramer-von Mises (CV) test [25]. The CV statistic is nothing but the integrated squared error between the empirical and theoretical distribution functions. To avoid the impact of having correlated samples [20], we first downsampled each record of $S_0(t)$ such that the correlation between any two adjacent samples was reduced to 0.5. The number of (approximately) uncorrelated samples varies between 8 and 22 over all the twelve records. Using these samples of $S_0(t)$, we estimated the parameters of the gamma and lognormal distributions via the method of maximum likelihood. We used the percentage points given in Table 4.21 of [25] for the CV statistics in testing the gamma distribution. For testing the lognormal distribution, we used the percentage points given in Table 4.7 of [25] for the modified CV statistics. The results of the test for all the twelve sets of data, at the significance level of 0.05, are listed in Table I of [26], in terms of the rejection or acceptance of the null hypothesis. According to this table, there seems to be no preference in choosing between the gamma PDF and the lognormal PDF for our data sets. The empirical distribution of $S_0(t)$ in some data records for which both gamma and lognormal hypotheses are accepted, are shown in Fig. 2. The associated gamma and lognormal distributions are also shown in Fig. 2, which are very close to each other.

A.2. Akaike Information Criterion

Akaike Information Criterion (AIC) can be used for model selection, by estimating the expected relative information distance between a model and the data [19]. It has also recently been used for channel modeling [27]. For each of the twelve records of measured data, the numerical values of AIC calculated for gamma and lognormal PDFs, i.e., AIC_g and AIC_l, respectively, are given in Table I. These are computed using the AIC expression provided in p. 61 of [19]. Since the relative value of AIC is important for model selection and not its absolute value [19], AIC differences are listed in Table I as well. For the gamma and lognormal PDFs we have, respectively, $\Delta_g = \mathrm{AIC}_g - \min(\mathrm{AIC}_g, \mathrm{AIC}_l)$ and $\Delta_l = \mathrm{AIC}_l - \min(\mathrm{AIC}_g, \mathrm{AIC}_l)$. As a rule of thumb, an AIC difference between 0 and 2 indicates substantial empirical support for the model [19]. Based on Table I, for nine out of twelve data sets, both gamma and lognormal PDFs are comparably good models. The close agreement between the gamma and lognormal distributions in Fig. 2 supports this observation.

A.3. Use of Published Data

To compare the gamma and lognormal distributions for other sets of terrestrial measurements, we have used the empirical path loss models and estimated shadow standard deviations to obtain some practical values for μ and σ, respectively. Specifically, we have used the two-slope street microcell path loss model, Eq. (2.248) [1], with its parameters taken from the bottom of p. 113 in [1], and also Lee's area-to-area macrocell path loss model, Eq. (2.233) [1], with its parameters computed under the nominal conditions. The numerical values of σ for the microcell and macrocell models are taken from p. 113 and p. 99 of [1], respectively. We have also used the empirical values of μ and σ obtained from extensive ultrawideband measurements and reported in Tables I, II, III, IV and IX [7]. These tables refer to residential, office, outdoor/farm, industrial and body area network, respectively. The corresponding parameters of the gamma distribution, Ω and ν, are calculated using the relations derived in [28]

$$\mu = \ln\left(\Omega/\nu\right) + \Psi(\nu), \quad \sigma^2 = \Psi'(\nu), \tag{3}$$

where $\Psi(.)$ and $\Psi'(.)$ are the psi function and its derivative, respectively [29]. In Fig. 3 and Fig. 4 we have plotted the distribution functions of gamma and lognormal for many different sets of parameters. We observe that the gamma and the lognormal distributions are close enough over a wide range of S_0 values and for different propagation environments.

B. Satellite Channels

For this type of channel, we have used the parameters of the lognormal distribution, estimated from a comprehensive set of data collected at many different places and elevation angles [8]. In Fig. 5 we have plotted the distribution functions of the gamma and lognormal distributions, with μ and σ taken from Table II of [8], whereas Ω and ν are computed using (3). As these figures show, the gamma and the lognormal distributions are reasonably close over the practical ranges of μ and σ.

It is noteworthy that if *X* has a gamma PDF, then the PDF of $\sqrt{X}$ is Nakagami [1]. On the other hand, if the PDF of *X* is modeled to be lognormal, then the PDF of $\sqrt{X}$ is lognormal as well. Therefore, equations similar to (3) can be derived to obtain the Nakagami parameters from lognormal parameters.

At the end of this section we briefly point out one possible wave propagation justification for the gamma PDF, based on the physics of wave scattering from random rough surfaces. According to [30], the density of rays, $\Re$, scattered by a Gaussian rough surface with differentiable height and fractal slope follows a gamma distribution. Here the fractal slope means that the structure function of the local random slope has a power-law form, with the power being related to the fractal dimension *D*. The shape parameter of the gamma PDF for ray density $\Re$ can be expressed in terms of *D* [30]. On the other hand, it is shown in [31] that stochastic variations of $\Re$ are equivalent to the random fluctuations of *N*, the number of scattered waves that are received via multiple paths. Since random fluctuations of *N* appear as random changes in the average power of the Rayleigh PDF [32] of the signal envelope, i.e., $E[R^2|N] \propto N$, then one can

conclude that the local average power has the same PDF as $\Re$. This suggests the use of gamma distribution for the received local average power, from a random wave scattering perspective.

III. System Performance Analysis

In this section we show how the application of the gamma distribution for shadow fading allows straightforward and convenient system performance analysis, with closed-form results and mathematically tractable solutions. The same system analysis procedures with the lognormal distribution most often end up with integrals that have to be solved numerically. In this paper we focus on the calculation of average symbol error rate in diversity receivers over multipath fading/shadow fading wireless channels. The reader should bear in mind that there are papers published in recent years that have analyzed the performance of diversity combiners for the *K* fading model and its extensions. Examples include [33]-[35]. So, some of the expressions below might have been presented in such papers, perhaps in different forms and in terms of different or related mathematical functions. The goal of this section, however, is to derive, from first principles, some performance prediction expressions that within the context of the paper can demonstrate the usefulness of gamma shadow fading model.

Let $R(t)$ denote the received signal envelope in the fading channel. As is discussed in [3], the moment generating function (MGF) of R^2, $\mathrm{M}_{R^2}(\xi) = E[\exp(-\xi R^2)]$, $\xi \geq 0$, and the characteristic function (CF) of R, $\Phi_R(\omega) = E[\exp(j\omega R)]$, $j^2 = -1$, play key roles in the performance analysis of multichannel reception schemes over generalized fading channels. To show this, we note that the power at the output of an *L*-branch maximal ratio combiner (MRC) can be written as $S_{out,MRC} = \sum_{i=1}^{L} R_i^2$, while for the envelope at the output of an *L*-branch equal gain combiner (EGC) we have $R_{out,EGC} = \sum_{i=1}^{L} R_i$ [3]. If the *L* branches are independent, then the MGF of $S_{out,MRC}$ and the CF of $R_{out,EGC}$, which we need for calculating the average symbol error rate of MRC and EGC, respectively [3], can be easily obtained by multiplying *L* MGFs and CFs, respectively. The function $\mathrm{M}_{R^2}(\xi)$, also named as the image function of *R*, is of significant importance in the performance analysis of mobile radio networks as well [36].

If we assume that multipath fading follows the Rayleigh distribution, then we obtain the composite Rayleigh-lognormal distribution (also known as Suzuki distribution), which is a common model for the signal envelope in both terrestrial [37] and satellite channels [8]. However, the functions $\mathrm{M}_{R^2}(\xi)$ and $\Phi_R(\omega)$ for the Rayleigh-lognormal model can be expressed only in terms of definite integrals, which cannot be expressed and/or simplified in terms of known mathematical functions. To show this, note that conditioned on S_0, the Rayleigh PDF of multipath fading is given by $f_R(r|S_0) = (2r/S_0)\exp(-r^2/S_0)$. It is easy to verify that $E[\exp(-\xi R^2)|S_0] = (1+\xi S_0)^{-1}$, while from p. 285 of [3], it can be shown that $E[\exp(j\omega R)|S_0] = D_{-2}(-j\omega\sqrt{S_0}/\sqrt{2})\exp(-S_0\omega^2/8)$, where $D_{-2}(.)$ is the parabolic cylinder function of order –2 [38]. According to the lognormal distribution of S_0 in (2), the functions $\mathrm{M}_{R^2}(\xi)$ and $\Phi_R(\omega)$ for the Rayleigh-lognormal model are

$$\mathrm{M}_{R^2}(\xi) = \frac{1}{\sqrt{2\pi\sigma^2}}\int_0^\infty \frac{\exp\left[-(\ln s_0 - \mu)^2/(2\sigma^2)\right]}{s_0(1+\xi s_0)}\, ds_0, \tag{4}$$

$$\Phi_R(\omega) = \frac{1}{\sqrt{2\pi\sigma^2}}\int_0^\infty s_0^{-1}\exp\left[-(\ln s_0 - \mu)^2/(2\sigma^2)\right]\exp(-s_0\omega^2/8) \\ D_{-2}(-j\omega\sqrt{s_0}/\sqrt{2})\, ds_0. \tag{5}$$

Because of the special mathematical form of the lognormal PDF, the integrals in (4) and (5) cannot be further simplified.

On the other hand, if we replace the lognormal model of shadow fading with the gamma model in (1), then the PDF of *R*, $f_R(r)$, and also $\mathrm{M}_{R^2}(\xi)$ and $\Phi_R(\omega)$ can be readily expressed in terms of tabulated functions. For $f_R(r)$ we obtain the *K* distribution [28][2]

---

[2] The equivalence of *K* and Suzuki PDFs is investigated in [28] using their moment generating functions. Here we compare their tails, since the low-side tail is related to signal outage whereas the high-side tail appears in interference studies. We have calculated some percentiles of these two PDFs, using the recent extensive measurements taken in many different environments to build a standardized model [7]. Since the measured values of the shadow mean, μ, mostly affect the locations of the distributions, we set μ to 0 dB. Let the PDF of *R*, the received signal envelope, be *K* or Suzuki. We define $r_{low}(\mathrm{dB})$ as the low-side tail such that $\Pr\{20\log R \le r_{low}(\mathrm{dB})\} = 0.01$, where log is logarithm to the base 10. Similarly,

$$f_R(r) = E_{S_0}\left[f_R(r|S_0)\right] = \frac{4}{\Gamma(\nu)}\left(\frac{\nu}{\Omega}\right)^{\frac{\nu+1}{2}} r^{\nu} K_{\nu-1}\left(\sqrt{\frac{4\nu}{\Omega}}\, r\right), \quad r \geq 0, \tag{6}$$

where $K_{\nu-1}(.)$ is the modified Bessel function of the second kind and order $\nu - 1$ [38]. Some binary error probability calculations for single branch receivers in *K*-distributed fading channels are presented in [39] and [40]. More results can be found in [33]-[35].

Under the assumption of gamma shadow fading, the MGF of R^2 can be obtained by averaging $E[\exp(-\xi R^2)|S_0] = (1+\xi S_0)^{-1}$ with respect to the gamma PDF of S_0 in (1)

$$\mathrm{M}_{R^2}(\xi) = \left(\frac{\nu}{\Omega\xi}\right)^{\nu} \exp\left(\frac{\nu}{\Omega\xi}\right) \Gamma\left(1-\nu, \frac{\nu}{\Omega\xi}\right), \tag{7}$$

where $\Gamma(.,.)$ is the incomplete gamma function, defined as $\Gamma(a,z) = \int_z^{\infty} e^{-t} t^{a-1} dt$ [38]. Moreover, by calculating the average of $\exp(j\omega R)$ with respect to the *K* PDF in (6), using Eq. (6.621-3) in p. 733 of [38], the CF of *R* can be written as

$$\Phi_R(\omega) = \frac{\sqrt{\pi}(4\nu)^{\nu}\,\Gamma(2\nu)}{\Gamma(\nu)\Gamma(\nu+3/2)}\left(2\sqrt{\nu} - j\sqrt{\Omega}\omega\right)^{-2\nu} F\left(2\nu, \nu-\frac{1}{2}, \nu+\frac{3}{2}, \frac{2\sqrt{\nu}+j\sqrt{\Omega}\omega}{-2\sqrt{\nu}+j\sqrt{\Omega}\omega}\right), \tag{8}$$

where $F(.,.,.,.)$ is the Gauss hypergeometric function [38]. Notice the clean and compact forms of equations (7) and (8) for the gamma model of shadow fading, compared to the integral forms of the expressions in (4) and (5) for the lognormal distribution. The mathematical properties of

---

$r_{high}(\mathrm{dB})$ is the high-side tail such that $\Pr\{20\log R > r_{high}(\mathrm{dB})\} = 0.01$. In ten out of eleven propagation scenarios [7], the difference between $r_{low}(\mathrm{dB})$ under two different models is at most 0.7 dB. Only for the industrial environment, with the large shadow standard deviation of $\sigma = 6$ dB, the difference is about 2.5 dB in the envelope level. For this large σ, the difference in $r_{high}(\mathrm{dB})$ for the two PDFs is 2.8 dB in the envelope level. In all other cases, the difference in $r_{high}(\mathrm{dB})$ is about or less than 1 dB. These numerical results are consistent with the analytical finding of [28], which says for large shadow standard deviation σ, some differences between the two models show up. The difference between the tails of the two distributions appears to be about or less than 1 dB in most of the cases and environments, where σ is not large [7].

$\Gamma(.,.)$ and $F(.,.,.,.)$ such as recursive relations, asymptotic expansions, etc., are extensively discussed in any standard book on special functions such as [29]. In addition, any standard mathematical software such as Mathematica or Matlab has built-in procedures for efficient numerical evaluation of these functions. These make the gamma distribution an attractive model for shadow fading, from a performance analysis point of view.

If the L branches are independent, then the MGF of $S_{out,MRC}$ and the CF of $R_{out,EGC}$ can be easily obtained by multiplying L terms according to (7) and (8), respectively. However, there are some cases of interest in which we can obtain much simpler closed-form solutions for the MGF or the CF of the output of the combiner. For example, consider an L-branch diversity combiner where the multipath Rayleigh components of the branches are independent, but all the branches experience a common local average power S_0 [5]. Let $S_{out,SC} = \max(R_1^2, R_2^2, ..., R_L^2)$ denote the power at the output of a selection combiner (SC) [5]. For the gamma distributed S_0 in (1), the MGF of $S_{out,MRC}$ and $S_{out,SC}$ in such a setting can be shown to be

$$\mathrm{M}_{S_{out,MRC}}(\xi) = \left(\frac{\nu}{\Omega\xi}\right)^{\nu} U\left(\nu, \nu - L + 1, \frac{\nu}{\Omega\xi}\right), \tag{9}$$

$$\mathrm{M}_{S_{out,SC}}(\xi) = 1 + \nu\left(\frac{\nu}{\Omega\xi}\right)^{\nu} \sum_{i=1}^{L} \frac{(-1)^i i^{\nu} L!}{(L-i)!\, i!}\ \Gamma\left(-\nu, \frac{i\nu}{\Omega\xi}\right) \exp\left(\frac{i\nu}{\Omega\xi}\right), \tag{10}$$

where $U(.,.,.)$ is the Tricomi function, defined in Eq. (48:3:5) of [41] as $U(a,c,z) = \Gamma(a)^{-1} \int_0^{\infty} t^{a-1} e^{-zt} (1+t)^{c-a-1} dt$ (also available in Mathematica). Using the relations $\Gamma(a,z) = \exp(-z) U(1-a, 1-a, z)$ and $\Gamma(a+1,z) = a\Gamma(a,z) + z^a \exp(-z)$ [38], it is easy to verify that for $L = 1$, both (9) and (10) simplify to (7), as expected. Needless to say, the lognormal model of shadow fading for S_0 results in integral expressions that cannot be written in terms of known mathematical functions [5].

In Fig. 6 we have plotted the average bit error rates of binary differential phase shift keying (BDPSK) modulation with MRC and SC, $L = 3$, assuming K and Suzuki fading models for two satellite channels with $\sigma = 2$ dB and $\sigma = 6$ dB. The bit error rate of BDPSK is calculated according to $\mathrm{M}_{S_{out}}(\gamma)/2$ [5], where γ is the signal-to-noise- ratio (SNR) per branch of the

unfaded link. Note that $\mathrm{M}_{S_{out}}(.)$ for the *K* model is given by (9) and (10) in simple closed forms, for both combiners. For the Suzuki model, we used the numerical integration routine of Mathematica to compute $\mathrm{M}_{S_{out}}(.)$. As Fig. 6 demonstrates, bit error rate curves are close enough over a wide range of SNRs.

To compare gamma and lognormal shadow fading models in terms of computational complexity, here we report the time it takes for Mathematica to compute about two hundred data points of each curve in Fig. 6. To calculate the performance of a maximal ratio combiner with BDPSK, for $\sigma = 6$ dB, the required time is 0.203 sec. and 0.75 sec. for *K* and Suzuki models, respectively. The required time when $\sigma = 2$ dB is 0.5 sec. and 0.922 sec., respectively. For a selection combiner with BDPSK and $\sigma = 6$ dB, it takes 0.062 sec. and 2.953 sec. to calculate the performance using *K* and Suzuki models, respectively. For $\sigma = 2$ dB, these timings change, respectively, to 0.141 sec. and 3.485 sec. Upon dividing the computation time for the Suzuki model by the *K* model computation time, we obtain a computational efficiency metric. If this metric is greater than one, it means the gamma-based model is computationally more efficient (faster), as it takes less time to compute the system performance using the gamma shadow fading model. For the cases listed above, the defined computational efficiency metric is 3.7, 1.8, 47.6 and 24.7, respectively. This indicates the gamma model is computationally more efficient. One possible reason is that Mathematica, and other mathematical/numerical softwares, typically have built-in optimized procedures for efficient numerical evaluation of many special functions, including those that may appear in system performance studies based on the gamma shadow fading model. Whereas for the lognormal model, softwares have to use general-purpose integration techniques, to numerically compute the integrals that arise in system performance studies using this model.

IV. CONCLUSION

In this paper and based on experimental data, we have demonstrated that the gamma distribution can model shadow fading in both terrestrial and satellite channels. Furthermore, we

have shown that the application of the gamma model introduces significant analytical and computational facilities in calculating the average symbol error rate of diversity receivers over wireless channels.

V. ACKNOWLEDGEMENT

We would like to express our gratitude to Dr. J. A. Barger for providing us with the data.

REFERENCES

[1] G. L. Stuber, *Principles of Mobile Communication*, 2nd ed., Boston, MA: Kluwer, 2001.

[2] F. Vatalaro and F. Mazzenga, "Statistical channel modeling and performance evaluation in satellite personal communications," *Int. J. Satell. Commun.*, vol. 16, pp. 249-255, 1998.

[3] M. K. Simon and M.-S. Alouini, *Digital Communication over Fading Channels: A Unified Approach to Performance Analysis*. New York: Wiley, 2000.

[4] D. Cygan, "Analytical evaluation of average bit error rate for the land mobile satellite channel," *Int. J. Sat. Commun.*, vol. 7, pp. 99-102, 1989.

[5] C. Tellambura, A. J. Mueller, and V. K. Bhargava, "Analysis of *M*-ary phase-shift keying with diversity reception for land-mobile satellite channels," *IEEE Trans. Vehic. Technol.*, vol. 46, pp. 910-922, 1997.

[6] H. Allen Barger, "Dynamic characteristics of a narrowband land mobile communication channel," *IEEE Trans. Vehic. Technol.*, vol. 47, pp. 216-224, 1998.

[7] A. F. Molisch, D. Cassioli, C.-C. Chong, S. Emami, A. Fort, B. Kannan, J. Karedal, J. Kunisch, H. G. Schantz, K. Siwiak and M. Z. Win, "A comprehensive standardized model for ultrawideband propagation channels," *IEEE Trans. Antennas Propag.*, vol. 54, pp. 3151-3166, 2006.

[8] E. Lutz, D. Cygan, M. Dippold, F. Dolainsky, and W. Papke, "The land mobile satellite communication channel – Recording, statistics, and channel model," *IEEE Trans. Vehic. Technol.*, vol. 40, pp. 375-386, 1991.

[9] A. Abdi and M. Kaveh, "On the utility of the gamma PDF in modeling shadow fading (slow fading)," in *Proc. IEEE Vehic. Technol. Conf.*, Houston, TX, 1999, pp. 2308-2312.

[10] D. Middleton, "New physical-statistical methods and models for clutter and reverberation: the KA-distribution and related probability structures," *IEEE J. Oceanic Eng.*, vol. 24, pp. 261-284, 1999.

[11] K. D. Ward, C. J. Baker, and S. Watts, "Maritime surveillance radar-Part 1: Radar scattering from the ocean surface," *IEE Proc. F, Radar, Signal Processing*, vol. 137, pp. 51-62, 1990.

[12] R. Barakat, "Second-order statistics of integrated intensities and of detected photoelectrons," *J. Modern Opt.*, vol. 34, pp. 91-102, 1987.

[13] C. Roberts and S. Geisser, "A necessary and sufficient condition for the square of a random variable to be gamma," *Biometrika*, vol. 53, pp. 275-278, 1966.

[14] A. Abdi, H. Allen Barger, and M. Kaveh, "A parametric model for the distribution of the angle of arrival and the associated correlation function and power spectrum at the mobile station," *IEEE Trans. Vehic. Technol.*, vol. 51, pp. 425-434, 2002.

[15] A. Abdi, H. A. Barger, and M. Kaveh, "Signal modeling in wireless fading channels using spherically invariant processes," in *Proc. IEEE Int. Conf. Acoust., Speech, Signal Processing*, Istanbul, Turkey, 2000, pp. 2997-3000.

[16] A. Abdi, K. Wills, H. A. Barger, M. S. Alouini, and M. Kaveh, "Comparison of the level crossing rate and average fade duration of Rayleigh, Rice, and Nakagami fading models with mobile channel data," in *Proc. IEEE Vehic. Technol. Conf.*, Boston, MA, 2000, pp. 1850-1857.

[17] W. C. Y. Lee and Y. S. Yeh, "On the estimation of the second-order statistics of lognormal fading in mobile radio environment," *IEEE Trans. Commun.*, vol. 22, pp. 869-873, 1974.

[18] R. B. D'Agostino and M. A. Stephens, Eds., *Goodness-of-Fit Techniques*. New York: Marcel Dekker, 1986.

[19] K. P. Burnham and D. R. Anderson, *Model Selection and Multimodel Inference: A Practical Information-Theoretic Approach*, 2nd ed., New York: Springer, 2002.

[20] L. J. Gleser and D. S. Moore, "The effect of dependence on chi-squared and empiric distribution tests of fit," *Ann. Statist.*, vol. 11, pp. 1100-1108, 1983.

[21] H. L. Crutcher, "A note on the possible misuse of the Kolmogorov-Smirnov test," *J. Appl. Meteor.*, vol. 14, pp. 1600-1603, 1975.

[22] P. Albrecht, "On the correct use of the chi-square goodness-of-fit test," *Scand. Actuarial J.*, vol. 1, pp. 149-160, 1980.

[23] P. Albrecht, "A remark on Albrecht's "On the correct use of the chi-square goodness-of-fit test"," *Scand. Actuarial J.*, vol. 3, pp. 168-170, 1982.

[24] D. S. Moore, "Tests of chi-squared type," in *Goodness-of-Fit Techniques*. R. B. D'Agostino and M. A. Stephens, Eds., New York: Marcel Dekker, 1986, pp. 63-95.

[25] M. A. Stephens, "Tests based on EDF statistics," in *Goodness-of-Fit Techniques*. R. B. D'Agostino and M. A. Stephens, Eds., New York: Marcel Dekker, 1986, pp. 97-193.

[26] A. Abdi, H. A. Barger, and M. Kaveh, "A simple alternative to the lognormal model of shadow fading in terrestrial and satellite channels," in *Proc. IEEE Vehic. Technol. Conf.*, Atlantic City, NJ, 2001, pp. 2058-2062.

[27] U. G. Schuster and H. Bolcskei, "Ultrawideband channel modeling on the basis of information-theoretic criteria," *IEEE Trans. Wireless Commun.*, vol. 6, pp. 2464-2475, 2007.

[28] A. Abdi and M. Kaveh, "*K* distribution: an appropriate substitute for Rayleigh-lognormal distribution in fading-shadowing wireless channels," *Electron. Lett.*, vol. 34, pp. 851-852, 1998.

[29] W. Magnus, F. Oberhettinger, and R. P. Soni, *Formulas and Theorems for the Special Functions of Mathematical Physics*, 3rd ed., New York: Springer, 1966.

[30] E. Jakeman, "Scattering by a corrugated random surface with fractal slope," *J. Phys. A: Math. Gen.*, vol. 15, pp. L55-L59, 1982.

[31] E. Jakeman, "Fresnel scattering by a corrugated random surface with fractal slope," *J. Opt. Soc. Am.*, vol. 72, pp. 1034-1041, 1982.

[32] E. Jakeman, "On the statistics of *K*-distributed noise," *J. Phys. A: Math. Gen.*, vol. 13, pp. 31-48, 1980.

[33] P. Theofilakos, A. G. Kanatas and G. P. Efthymoglou, "Performance of generalized selection combining receivers in *K* fading channels," *IEEE Commun. Lett.*, vol. 12, pp. 816-818, 2008.

[34] P. S. Bithas, P. T. Mathiopoulos and S. A. Kotsopoulos, "Diversity reception over generalized-*K* (K_G) fading channels," *IEEE Trans. Wireless Commun.*, vol. 6, pp. 4238-4243, 2007.

[35] P. M. Shankar, "Performance analysis of diversity combining algorithms in shadowed fading channels," *Wireless Personal Commun.*, vol. 37, pp. 61-72, 2006.

[36] J. P. Linnartz, *Narrowband Land-Mobile Radio Networks*. Boston, MA: Artech House, 1993.

[37] J. D. Parsons, *The Mobile Radio Propagation Channel*. New York: Wiley, 1992.

[38] I. S. Gradshteyn and I. M. Ryzhik, *Table of Integrals, Series, and Products*, 5th ed., A. Jeffrey, Ed., San Diego, CA: Academic, 1994.

[39] A. Abdi and M. Kaveh, "Comparison of DPSK and MSK bit error rates for *K* and Rayleigh-lognormal fading distributions," *IEEE Commun. Lett.*, vol. 4, pp. 122-124, 2000.

[40] M. Nesenbergs, "Binary error probability due to an adaptable fading model," *IEEE Trans. Commun. Syst.*, vol. 12, pp. 64-73, 1964.

[41] J. Spanier and K. B. Oldham, *An Atlas of Functions*. Washington: Hemisphere, 1987.

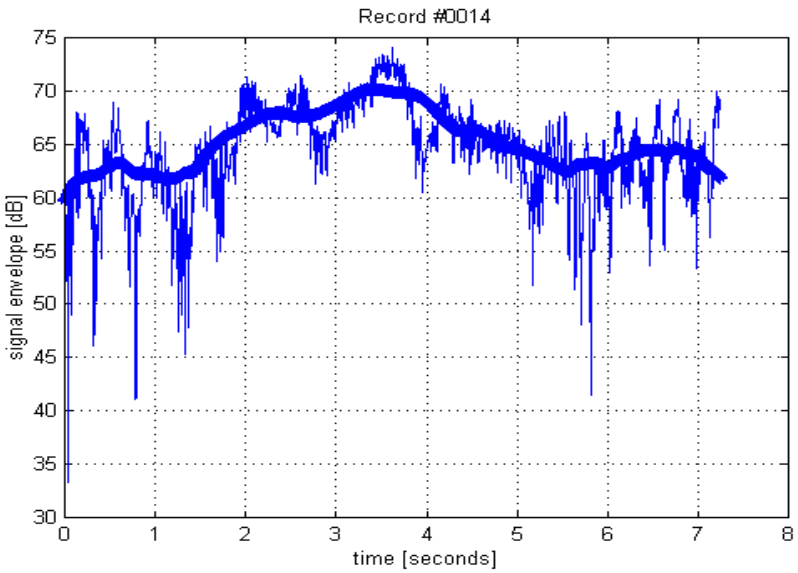

Fig. 1. The envelope $R(t)$ of record #0014, collected in a terrestrial channel in a suburban area. The bold slowly-varying signal is the square root of the running mean of the envelope squared, $\sqrt{S_0(t)}$.

Table I. AIC AND AIC DIFFERENCES OF GAMMA AND LOGNORMAL PDFS FOR THE SHADOW FADING COMPONENT OF DATA COLLECTED IN TERRESTRIAL CHANNELS

Record No.	AIC_g	AIC_l	Δ_g	Δ_l
0011	548.338	545.105	3.233	0
0012	243.946	243.01	0.936	0
0013	297.719	299.559	0	1.84
0014	324.794	324.167	0.627	0
0015	200.9048	200.808	0.0968	0
0016	270.846	269.931	0.915	0
0017	334.798	334.4	0.398	0
0018	396.874	398.236	0	1.362
0019	411.296	415.585	0	4.289
0020	309.848	308.462	1.386	0
0021	382.47	375.35	7.12	0
0022	467.93	468.98	0	1.05

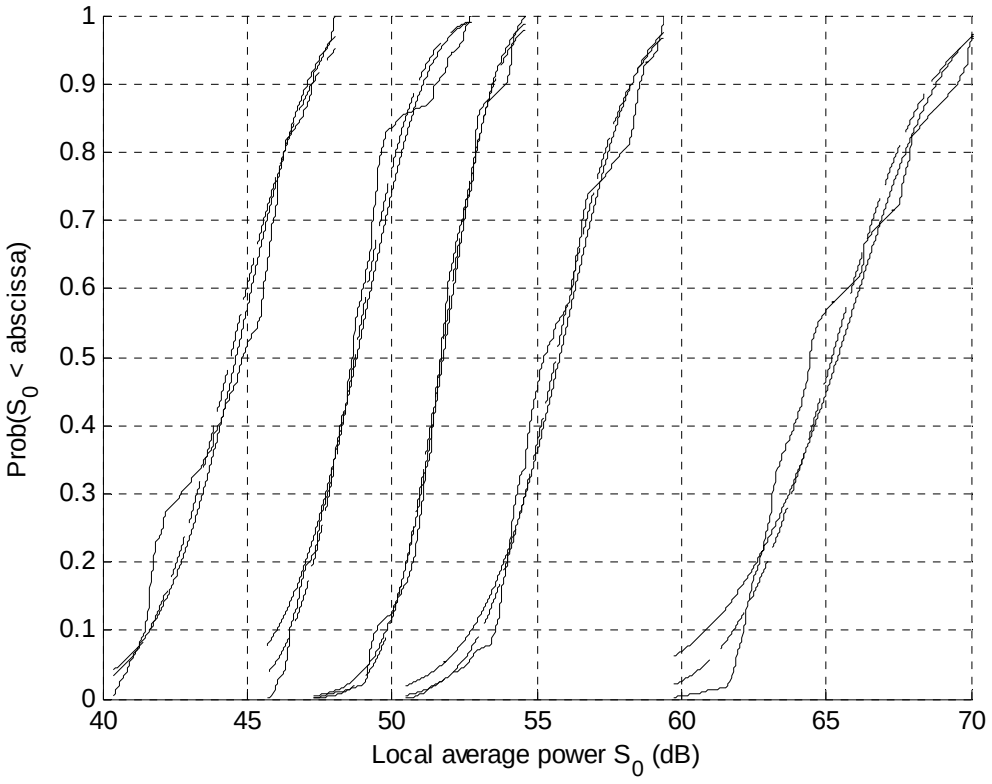

Fig. 2. Comparison of gamma and lognormal distributions using the collected terrestrial channel data (records #0014, #0015, #0016, #0018, #0020). Continuous irregular curves: empirical distributions, continuous monotone curves: gamma distributions, dashed curves: lognormal distributions.

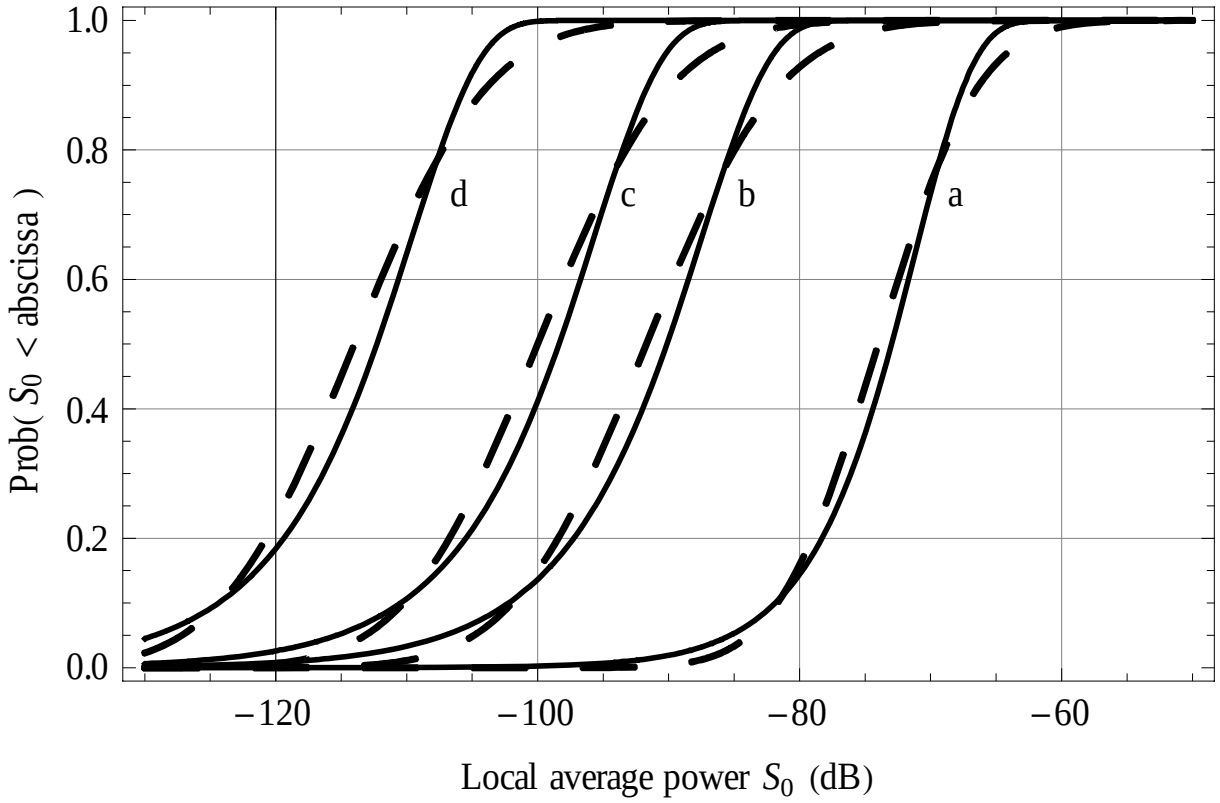

Fig. 3. Comparison of gamma and lognormal distributions in terrestrial channels. Continuous curves: gamma distributions, dashed curves: lognormal distributions.

(a) Street microcell, $\mu = -44$ dBm, $\sigma = 6$ dB, $\Omega = 7.6\times10^{-8}$, $\nu = 0.9$.

(b) North American suburban macrocell, $\mu = -61.7$ dBm, $\sigma = 8$ dB, $\Omega = 1.8\times10^{-9}$, $\nu = 0.62$.

(c) North American urban macrocell (Philadelphia), $\mu = -70$ dBm, $\sigma = 8$ dB, $\Omega = 2.7\times10^{-10}$, $\nu = 0.62$.

(d) Japanese urban macrocell (Tokyo), $\mu = -84$ dBm, $\sigma = 8$ dB, $\Omega = 1.1\times10^{-11}$, $\nu = 0.62$.

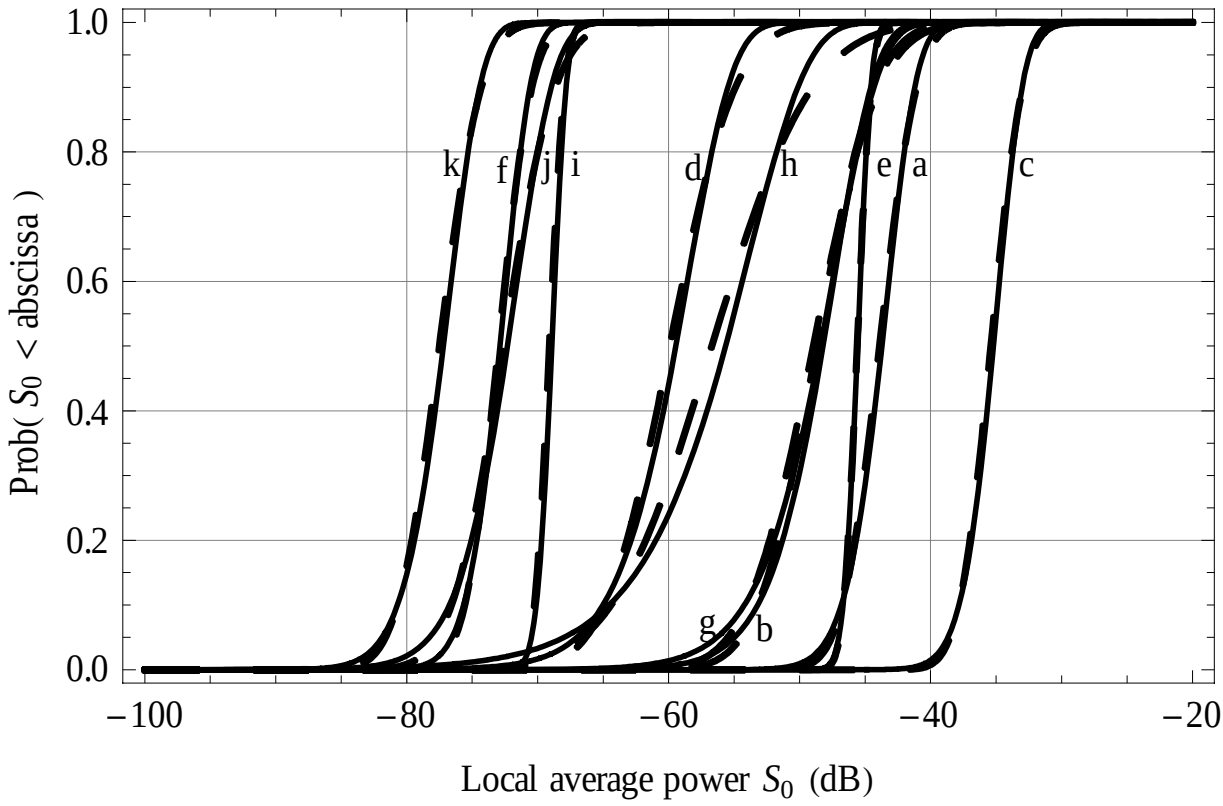

Fig. 4. Comparison of gamma and lognormal distributions in ultrawideband systems. Continuous curves: gamma distributions, dashed curves: lognormal distributions. The following tables refer to [7]. The numerical values listed for μ and σ are all in dB. LOS and NLOS stand for line-of-sight and non-line-of-sight, respectively.

(a) Residential, LOS (Table I): $\mu = -43.9,\ \sigma = 2.22,\ \Omega = 4.6\times10^{-5},\ \nu = 4.3.$

(b) Residential, NLOS (Table I): $\mu = -48.7,\ \sigma = 3.51,\ \Omega = 1.8\times10^{-5},\ \nu = 2.$

(c) Office, LOS (Table II): $\mu = -35.4,\ \sigma = 1.9,\ \Omega = 3.2\times10^{-4},\ \nu = 5.7.$

(d) Office, NLOS (Table II): $\mu = -59.9,\ \sigma = 3.9,\ \Omega = 1.4\times10^{-6},\ \nu = 1.7.$

(e) Outdoor, LOS (Table III): $\mu = -45.6,\ \sigma = 0.83,\ \Omega = 2.8\times10^{-5},\ \nu = 27.9.$

(f) Outdoor, NLOS (Table III): $\mu = -73,\ \sigma = 2,\ \Omega = 5.5\times10^{-8},\ \nu = 5.2.$

(g) Farm (Table III): $\mu = -48.96,\ \sigma = 3.96,\ \Omega = 1.8\times10^{-5},\ \nu = 1.6.$

(h) Industrial, LOS and NLOS (Table IV): $\mu = -56.7,\ \sigma = 6,\ \Omega = 4.1\times10^{-6},\ \nu = 0.9.$

(i) Body area network, Front (Table IX): $\mu = -69.1,\ \sigma = 0.9,\ \Omega = 1.3\times10^{-7},\ \nu = 24.$

(j) Body area network, Side (Table IX): $\mu = -72.6,\ \sigma = 3.1,\ \Omega = 6.8\times10^{-8},\ \nu = 2.4.$

(k) Body area network, Back (Table IX): $\mu = -77.5,\ \sigma = 2.5,\ \Omega = 2.1\times10^{-8},\ \nu = 3.5.$

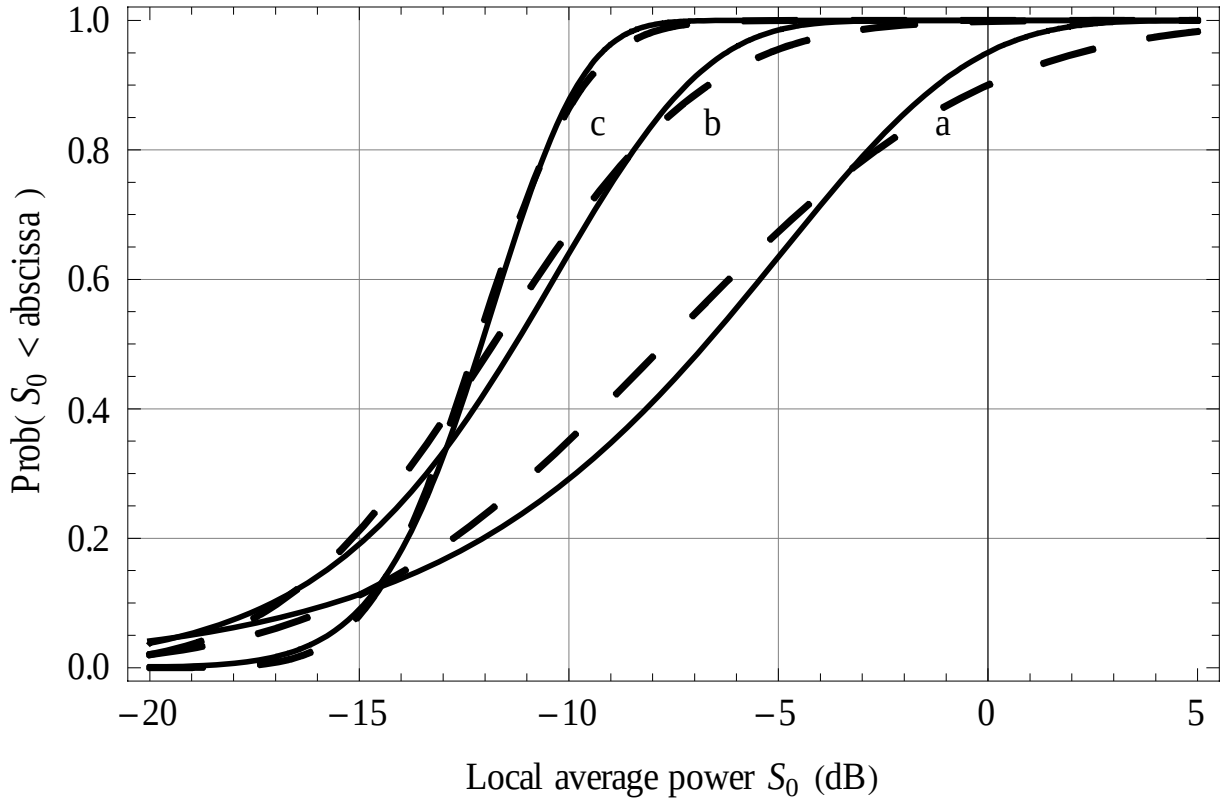

Fig. 5. Comparison of gamma and lognormal distributions in satellite channels. Continuous curves: gamma distributions, dashed curves: lognormal distributions.

(a) Data collected in a highway with the satellite elevation angle equal to 24°, $\mu = -7.7$ dB, $\sigma = 6$ dB, $\Omega = 0.32$, $\nu = 0.9$.

(b) Data collected in a city with the satellite elevation angle equal to 18°, $\mu = -11.8$ dB, $\sigma = 4$ dB, $\Omega = 0.093$, $\nu = 1.6$.

(c) Data collected in a city with the satellite elevation angle equal to 34°, $\mu = -12.2$ dB, $\sigma = 2$ dB, $\Omega = 0.066$, $\nu = 5.2$.

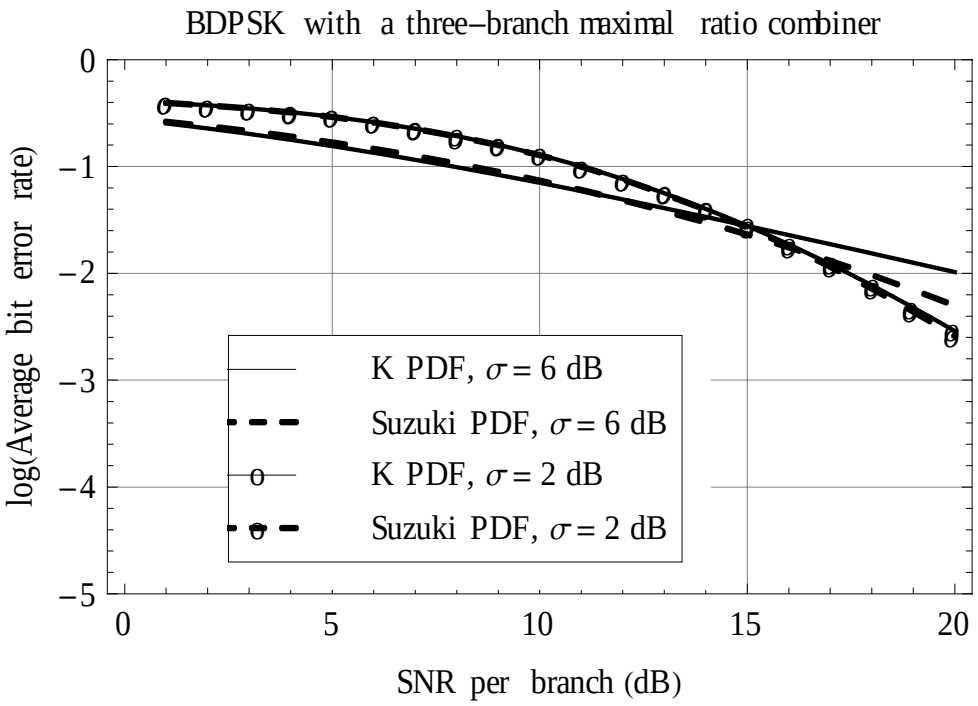

Fig. 6 (a) BDPSK modulation with a three-branch maximal ratio combiner.

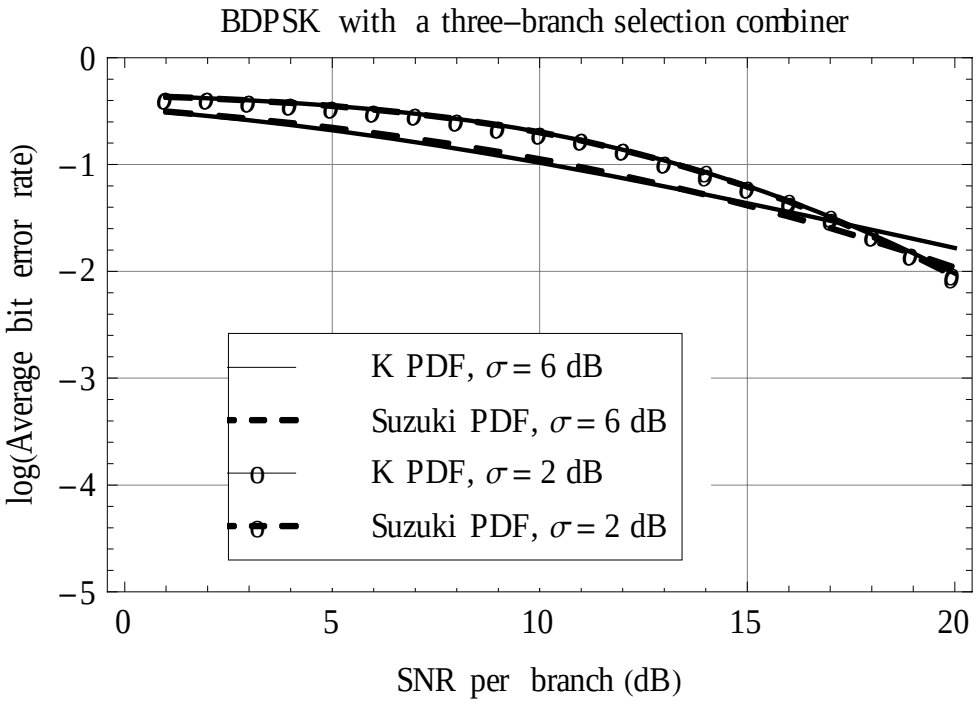

Fig. 6 (b) BDPSK modulation with a three-branch selection combiner.

Fig. 6. Comparison of the average bit error rates of BDPSK modulation in a maximal ratio combiner and a selection combiner, for K and Suzuki fading satellite channels. The numbers in the legend boxes refer to (1) data collected in a city with the satellite elevation angle equal to 34^{o}, $\mu = -12.2$ dB, $\sigma = 2$ dB, $\Omega = 0.066$, $\nu = 5.2$, and (2) data collected in a highway with the satellite elevation angle equal to 24^{o}, $\mu = -7.7$ dB, $\sigma = 6$ dB, $\Omega = 0.32$, $\nu = 0.9$.